

Demonstrating a new ink material for aerosol printing conductive traces and custom strain gauges on flexible surfaces

Dilan Ratnayake, Alexander Curry and Kevin Walsh

Department of Electrical and Computer Engineering

University of Louisville, Louisville, KY, USA

Email: d0ratn01@louisville.edu

Abstract— Aerosol Jet Printing is an emerging technology that holds much promise for the future of printable electronics and smart additive manufactured structures. Aerosol Jet Printers are capable of printing conformally on nearly any substrate due to their non-contact printing process and compatibility with a wide range of materials. These qualities allow these machines to be extremely versatile and capable of printing antennas, sensors, or even just conductive traces on PCBs and a wide variety of substrates. In this paper, a strain gauge sensor is designed and characterized using a new silver ink material from NovaCentrix and compared to a commercial off-the-shelf strain gauge. This work is the first to characterize the JS-A426 silver ink from NovaCentrix and demonstrate an application using an ultrasonic atomizer aerosol jet delivery system. After experimentally determining the conductivity of the silver ink, the length and area of the strain gauge were chosen to design a sensor with a theoretical resistance of 110 Ω . After aerosol printing and testing the printed strain gauge, it was found to have an average resistance of 116 Ω and a gauge factor of 1.85. These values are similar to commercial strain gauges and demonstrate that the aerosol printed strain gauge is a viable sensor that holds many advantages over traditional strain gauges: quick prototyping, conformally printed on any surface, elimination of any adhesive layer, and can be printed in less than a minute once the printer is setup.

Keywords—*Aerosol Jet Printing, Optomec, sintering, conductivity, strain gauge, Van der Pauw, gauge factor*

I. INTRODUCTION

Aerosol Jet Printing (AJP) works by placing specially formulated ink into either an ultrasonic or pneumatic atomizer that excites the liquid ink into a dense mist. Pressure forces the mist to travel to the deposition head where it becomes focused by a controlled sheath gas, usually nitrogen. As the aerosol stream and gas pass through the nozzle, they form a tight beam and begin to accelerate. This high velocity stream remains in tight formation from the nozzle all the way to the substrate, which is typically 2-5 mm away from the nozzle [1,2]. This standoff distance allows AJPs to print conformally on nearly any surface. The AJP process can print features as small as 10 microns all the way up to over a millimeter [3,4]. This is achieved by utilizing different nozzle sizes as well as varying the process parameters such as the atomizer flow rate and

sheath flow rate. AJP is also compatible with a wide range of materials – from polymers to conductive metals. This versatility of different feature sizes as well as material selection makes these printers extremely useful machines.

This study used an Aerosol Jet Print Engine with a Decathlon Print Cassette from Optomec for all printing processes. An ultrasonic atomizer was used to atomize a silver ink made by NovaCentrix. This study presents all the details for printing the new ink, sintering it, characterizing its conductivity, and using it for the design of conductive traces and custom strain gauges. These printable strain gauges are preferred because they solve a problem of commercial strain gauges – the need to attach the strain gauge to a device using some form of adhesive. Printable strain gauges can be incorporated directly onto a device in a single process. Although previous works have aerosol jet printed a strain gauge using a different NovaCentrix ink, they used a pneumatic atomizer and only achieved line widths of 160 μm and a gauge factor of 1.04 [5]. Our strain gauge allows for more flexible design since it contains line widths of 50 μm and achieves a larger gauge factor.

II. MATERIALS AND METHODS

A. Optomec Aerosol Print Engine System

The system is comprised of a print engine, a process control cabinet, and the KEWA process control software. A Velmex XY stage was used to control the motion. This Optomec AJP is equipped with a 300 μm diameter nozzle that allows features to be printed that are a tenth of the diameter, or 30 μm . This AJP uses an ultrasonic atomizer instead of a pneumatic atomizer. The ultrasonic atomizer works with inks that have a viscosity of around 1-10 cP. It is crucial that the materials chosen remain within this viscosity, otherwise the ink will not atomize, and the system will not be able to output material. Fig. 1 shows some examples of narrow prints on different surface features – a 35 μm width printed line on a glass slide (a), a 55 μm width printed line on a glass slide (b), a strain gauge printed on a glass wafer (c) and a strain gauge printed on a Kapton sheet (d). NovaCentrix JS-A426 silver ink was used throughout all printing and the process recipes were optimized/tuned by changing the sheath flow rate, atomizer flow rate, substrate

material, stand-off distance and stage speed in order to change the morphology of the printed lines.

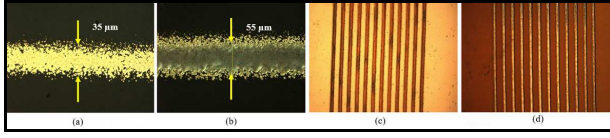


Fig. 1. 35 μm width printed line on a glass slide (a), 55 μm width printed line on a glass slide (b), strain gauge printed on a glass wafer (c) and strain gauge printed on a Kapton sheet (d)

B. Strain Gauge Design

The strain gauge for this study was designed using 50 μm wide traces because that width is easily achievable using the Optomec with a 300 μm nozzle. Having measured the conductivity of the NovaCentrix silver ink to be around $7.05 \times 10^6 \text{ S/m}$, the strain gauge target resistance was chosen to be around 110 Ω . Equation (1) below was used to design the dimensions of the strain gauge.

$$R = \rho(L/A) \quad (1)$$

In equation (1), R is the overall resistance of the strain gauge, L is the composite length of the meandering trace, A is the cross-sectional area of an individual trace, and ρ is the average resistivity of the material. Fig. 2 (a) shows the final design of the gauge with an overall trace width of 1.7mm and length of 4mm.

C. Printing Process

For this strain gauge design, the parameters chosen for the Optomec need to yield continuous, 50 μm -width lines. To achieve traces this thin, it is necessary to increase the sheath flow rate to shrink the aerosol beam. The following parameters, shown in Table 1, were set in the KEWA process control software to meet the design specifications for the strain gauge:

TABLE 1. PROCESS PARAMETERS

Sheath Flow Rate	135 sccm	Atomizer Current	500 mA
Atomizer Flow Rate	15 sccm	Print Speed	10 mm/s
Divert and Boost	30 sccm	Ultrasonic Atomizer Bath	23 °C

It is important to note that these parameters are unique to the specific ink chosen - the JS-A426 silver nanoparticle ink from NovaCentrix. Other inks may require different settings to yield the same results. Additionally, the ink was diluted with a 2:1 ratio of ink to DI water. The total volume of ink and DI water used was 3 ml. After the process stabilized and initial traces were examined using a microscope to be close to 50 μm wide, the strain gauge design was printed on a Kapton substrate as shown in Fig. 2 (b).

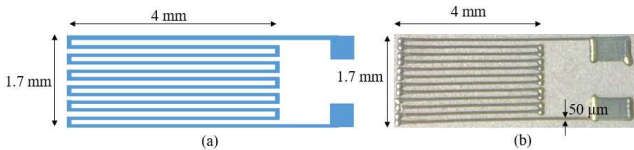


Fig. 2. Strain gauge design (a) and Printed strain gauge with dimensions (b)

D. Sintering Process

For this experiment, thermal curing using an oven was utilized to post-process the printed silver ink. There are several

other methods to sinter printed silver traces; however, thermal curing using an oven is one of the most reliable and consistent processes to do so. Thermal curing allows the solvent to evaporate and the silver nanoparticles to expand and fuse to each other, increasing the conductivity. The temperature can sometimes be constrained by the substrate choice, but this was not an issue for the Kapton. The printed strain gauge was cured at 200 °C for 24 hours.

E. Characterizing the Strain Gauge

Strain gauges which are typically made from thin metal wires or films, are used as sensors in systems to measure forces, moments, and the deformations of structures and materials. When the metal trace of a strain gauge is stretched with a parallel force, a dimensional change occurs in the trace, which causes L to increase, A to decrease, and its overall resistance to consequently increases, according to equation (1). This assumes the material's resistivity is independent of the strain, as is the case with most metals.

The primary figure of merit of a strain gauge is its "gauge factor" or GF, which is a measure of how sensitive the device is to a given applied strain. The equation for GF is provided below [6]:

$$GF = (\Delta R/R) / \epsilon \quad (2)$$

Where GF is the gauge factor, ϵ is the applied strain, R is the device's nominal resistance under no loading conditions, and ΔR is the measured change in resistance to the applied strain. As described in equation (2), if we know the strain and the corresponding change in resistance, the GF can be calculated. Let us consider the simple cantilever beam shown in Fig. 3. When a force F at the end of the beam is applied, the top of the beam will experience tension and the bottom of the beam will experience compression. Therefore, the strain gauge on top of the beam will be stretched, inducing a positive strain and thus a positive ΔR . We will use this process to determine the strain in the cantilever beam. An equation (given below) [7] can be used to calculate the theoretical strain on the surface of the beam at the location of the gauges.

$$\epsilon = (3dL_1t)/(2(L_2)^3) \quad (3)$$

Where d is the deflection of the beam and other parameters in the equation are shown in Fig. 3. For additional verification, a calibrated reference strain gauge with known GF can be positioned next to the device under test (DUT) to confirm the strain.

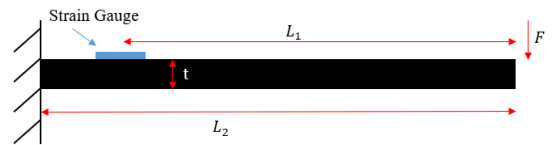


Fig. 3. Schematic of the cantilever beam with a strain gauge

This study uses both methods to determine the strain. A strain gauge characterization station from VISHAY Research Education was used to setup the metal beam and the strain gauges. A digital micrometer was used to apply the deflection and a high-quality digital multimeter was used to find the change in resistance.

III. RESULTS AND DISCUSSION

To determine the conductivity of the NovaCentrix silver ink, 3x3mm Van der Pauw square pads were printed on a 2-inch glass slide using a shadow mask. After printing, the Van der Pauw silver pads were sintered in the oven at 200 °C for 24 hours. Resistivity was measured using a probe station equipped with 4 micromanipulator probes and the average thickness of each pad was determined using a Dektak profilometer. Afterwards, the conductivity (σ) value was determined using equation (4) [8] and the resulting value (7.05×10^6 S/m) was used to design the strain gauge as discussed previously.

$$\sigma = (4.53)(h)(R) \quad (4)$$

Where h is the thickness of the pad and R is the average resistance. Next, the resistance of the printed strain gauge was determined using a high-quality digital multimeter. The gauge resistance was measured to be 116 Ω - very close to the designed specification of 110 Ω .

After measuring the resistance, the gauge was mounted on a metal beam and a reference strain gauge with a known GF (2.145) (resistance: 350 Ω) was mounted directly next to it, as shown in Fig. 4 (a). Then a digital micrometer was used to apply a deflection to the end of the metal beam shown in Fig. 4 (b). Before starting the experiment, the dimensions of the cantilever beam were measured using a ruler and a micrometer to calculate the theoretical strain using equation (4). Next, the metal beam was deflected in 0.25 mm increments using the micrometer until a total deformation of 2.5 mm was achieved. The changes in resistance corresponding to the changes in deformation were recorded using the digital multimeter for the reference strain gauge. Table 2 shows the theoretical and experimental strain, and both sets of data match up very well.

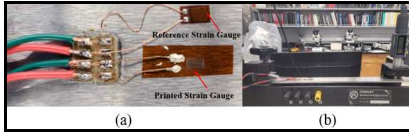


Fig. 4. Mounted printed and reference strain gauge on metal beam (a) and strain gauge measuring setup with micrometer (b)

TABLE 2. EXPERIMENTAL AND THEORATICAL STRAIN DATA

d (mm)	ΔR (ohms)	$\Delta R / R$	Strain(ϵ):Exp	Strain(ϵ):Theory
0.00	0.000	0.000E+00	0.00E+00	0.00E+00
0.25	0.010	2.848E-05	1.33E-05	1.33E-05
0.50	0.020	5.696E-05	2.66E-05	2.65E-05
0.75	0.030	8.545E-05	3.98E-05	3.98E-05
1.00	0.040	1.139E-04	5.31E-05	5.30E-05
1.25	0.050	1.424E-04	6.64E-05	6.63E-05
1.50	0.059	1.680E-04	7.83E-05	7.95E-05
1.75	0.068	1.937E-04	9.03E-05	9.28E-05
2.00	0.078	2.222E-04	1.04E-04	1.06E-04
2.25	0.087	2.478E-04	1.16E-04	1.19E-04
2.50	0.097	2.763E-04	1.29E-04	1.33E-04

Finally, the same procedure was done for our printed strain gauge to determine its GF. The change in resistance that corresponded to beam deflection was recorded and compiled in Table 3. Since both the experimental and theoretical strain data are very similar, we decided to use the experimental strain data from Table 2 to determine the GF of the printed strain gauge. Change in resistance with respect to initial resistance vs. strain

was plotted as shown Fig. 5 and the device's GF was determined using the gradient of the graph, which was 1.85.

TABLE 3. EXPERIMENTAL DATA FOR PRINTED STRAIN GAUGE

d (mm)	ΔR (ohms)	$\Delta R / R$	Strain(ϵ):Exp
0.00	0.000	0.000E+00	0.00E+00
0.25	0.004	3.112E-05	1.33E-05
0.50	0.007	5.445E-05	2.66E-05
0.75	0.010	7.779E-05	3.98E-05
1.00	0.013	1.011E-04	5.31E-05
1.25	0.016	1.245E-04	6.64E-05
1.50	0.019	1.478E-04	7.83E-05
1.75	0.022	1.711E-04	9.03E-05
2.00	0.025	1.945E-04	1.04E-04
2.25	0.028	2.178E-04	1.16E-04
2.50	0.031	2.411E-04	1.29E-04

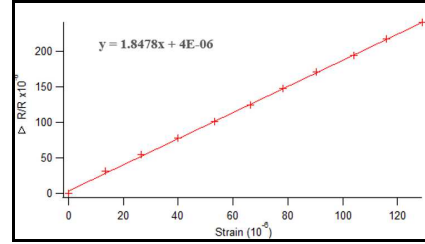


Fig. 5. ($\Delta R/R$) vs. strain for printed strain gauge

IV. CONCLUSION

This study investigated a new silver ink from NovaCentrix (JS-A426) for its potential application to be deposited on flexible substrates using aerosol jet printing. An Optomec Decathlon print engine was tuned to produce reliable 50 μm -width lines of this ink formulation over a relatively large area. We demonstrated that this process was very effective for producing both conductive traces and strain gauges. Oven sintering was used to cure the material at 200 °C for 24 hours. The Van der Pauw method was used to characterize the conductivity of the aerosol printed material and the final sintered films had a conductivity of 7.05×10^6 S/m, which is relatively close to that of bulk silver (6.3×10^7 S/m). Such a low resistivity allows these films to be used as effective conductive traces. Finally, we demonstrated that these films could also be used as in-situ potential strain gauges on flexible substrates. Using the same processing parameters, we designed miniature strain gauges with 50 μm traces and printed them on flexible Kapton films. Using a Vishay cantilever beam test setup and a calibrated commercial strain gauge, we characterized our aerosol printed strain gauge and determined its gauge factor to be 1.85, thus making printed gauges competitive potential sensors for a variety of unique applications.

V. ACKNOWLEDGMENT

This research was supported by National Science Foundation Award ECCS- 2025075 which is part of the NSF National Nanotechnology Coordinated Infrastructure (NNCI) and National Science Foundation Award ECCS-1828355 which is a part of MRI (Development of a Multiscale Additive Manufacturing Instrument with Integrated 3D Printing and Robotic Assembly).

REFERENCES

- [1] OPTOMECA, *AEROSOL JET PRINTED ELECTRONICS OVERVIEW*.
- [2] Hedges, M. and Marin, A.B., 2012, March. 3D Aerosol jet printing- Adding electronics functionality to RP/PM. In *DDMC 2012 conference* (pp. 1-5).
- [3] Rahman, T., et al., Aerosol based direct-write micro-additive fabrication method for sub-mm 3D metal-dielectric structures. *Journal of Micromechanics and Microengineering*, 2015. **25**(10): p. 107002.
- [4] Christenson, K.K., et al. *Direct printing of circuit boards using Aerosol Jet®*. in *NIP & Digital Fabrication Conference*. 2011. Society for Imaging Science and Technology.
- [5] M. Borghetti and E. Cantù, "Preliminary Study on a Strain Sensor Printed on 3D-plastic Surfaces for Smart Devices," *2019 II Workshop on Metrology for Industry 4.0 and IoT (MetroInd4.0&IoT)*, 2019, pp. 249-253, doi: 10.1109/METROI4.2019.8792896.
- [6] Beckwith, T.G., Buck, N.L. and Roy, D., Marangoni. 1982. *Mechanical Measurements*. Chapter 9.
- [7] Whitefoot, J., *Use of Strain Gages to Determine the Strain in Cantilever Beams*. 2018.
- [8] Philips'Gloeilampenfabrieken, O., *A method of measuring specific resistivity and Hall effect of discs of arbitrary shape*. Philips Res. Rep, 1958. **13**(1): p. 1-9.